Applied Catalysis B: Environmental 337 (2023) 122986

Contents lists available at ScienceDirect

Applied Catalysis B: Environmental

journal homepage: www.elsevier.com/locate/apcatb

Deconvoluting the roles of polyolefin branching and unsaturation on depolymerization reactions over acid catalysts

Ana Carolina Jerdy [a], Luis Trevisi [a], Masud Monwar [b], Miguel Ángel González-Borja [c], Ron Abbott [d], Lance Lobban [a], Steven Crossley [a,*]

[a] School of Chemical, Biological and Materials Engineering, University of Oklahoma, Norman, OK 73019, USA
[b] Chevron Phillips Chemical, Bartlesville, OK 74004, USA
[c] Chevron Phillips Chemical, Kingwood, TX 77339, USA
[d] Chevron Phillips Chemical, The Woodlands, TX 77380, USA

ARTICLE INFO

Keywords:
Polyethylene
Plastic upcycling
Chemical recycling
Branching
Unsaturation

ABSTRACT

Developing a circular economy for plastics is a societal priority with a range of stakeholders engaged in developing pathways to mechanical and chemical recycling. Acid catalysis has been proposed as an attractive strategy to chemically recycle or upcycle plastic waste. In principle, the energetics that govern polyolefin decomposition reactions over Brønsted acid sites should be the same ones known for alkane cracking. However, the nature of polymers as feedstock imposes new challenges for these well-known processes, e.g., strong mass transfer limitations. To better understand the role of polymer structure and diffusion on cracking rates, the effect of tertiary carbons, chain unsaturation, and catalyst active sites distribution were studied. Our findings confirm that higher concentrations of tertiary carbons will govern decomposition reactions, regardless of diffusion limitations. Also, we unveil that LLDPE reactions mostly take place on the external surface of ZSM-5 crystals while HDPE conversion takes place within the zeolite pores.

1. Introduction

Addressing plastic waste and shifting from a linear to a circular economy are growing environmental priorities worldwide. To tackle this problem, various approaches – pyrolysis, hydrogenolysis, hydrocracking, catalytic cracking, among others – have been proposed to convert plastic waste into monomers (recycling) or even more valuable streams (upcycling) [1–7]. Although the chemistry of catalytic polymerization has been studied for several decades [8], the field of depolymerization is much less explored and has only gained a great deal of attention in the past few years [9]. Catalytic decomposition of waste plastic presents new challenges – and opportunities – to the industry. Important questions include whether macromolecules will readily react over catalysts that were traditionally designed to convert much smaller molecules, and what polymer properties govern such reactions.

Regarding non-catalytic pyrolysis, high density polyethylene (HDPE) and low density polyethylene (LDPE) generally display similar decomposition curves, but HDPE tends to require slightly higher temperatures to be decomposed [10]. Marcilla et al. compared the reactivity of HDPE and LDPE over ZSM-5, and found that LDPE decomposed at faster rates [11]. This result was attributed to the fact that LDPE branches were able to penetrate the zeolite pores, thus increasing the activity. Uddin et al. also reported that LDPE and linear low density polyethylene (LLDPE) degraded at faster rates than HDPE over solid acid catalysts [12].

Zeolites have been extensively researched as catalysts to decompose polymers into short chain molecules [5,13–16]. It is important to notice that these are microporous materials, which, along with the fact that polymers are macromolecules and form highly viscous melts, implies strong mass transfer constraints [17]. The structural properties of polyolefins, such as the branching degree and their length, can play an important role in granting access to different active sites in microporous catalysts. Aguado et al. showed that nanocrystalline ZSM-5 presented enhanced activity for polyethylene conversion when compared to standard ZSM-5 [18], indicating that higher external surface area, and its consequent enhancement in diffusion, is an important factor for polyolefin conversion.

The mechanisms by which polyolefin upcycling reactions happen over a porous acid catalyst surface should be governed by the same

* Corresponding author.
E-mail address: stevencrossley@ou.edu (S. Crossley).

https://doi.org/10.1016/j.apcatb.2023.122986
Received 4 April 2023; Received in revised form 26 May 2023; Accepted 9 June 2023
Available online 10 June 2023
0926-3373/© 2023 Published by Elsevier B.V.

energetics that define alkane cracking, due to their similar chemical nature. Polymers are, however, orders of magnitude higher in molecular weight than alkanes commonly studied in the literature. Hence, polymer decomposition reactions are expected to be heavily influenced by external and internal diffusion limitations, and the influence that double bonds and tertiary carbons actually exert on the reaction rates should be reassessed for such molecules. One may expect that the presence of branches in polyethylene will enhance rates of cracking over acid catalysts, since tertiary carbons are known to generate more stable transition states when compared to secondary carbons [19]. However, branches will also hinder diffusion of the main polymer chain into the catalyst pores – on the other hand, if they are long enough, branches may separately diffuse into different pores.

The inherent presence of double bonds would also be expected to increase reaction rates over acid catalysts, since the activation energy for protonating olefins is lower than that for protonating paraffins due to higher proton affinities [20]. Conk et al. have recently demonstrated partial dehydrogenation of polyethylene as a strategy to induce C-C bond cleavage, providing a promising pathway to produce propylene from waste plastic [21].

Finally, another factor that will influence the rates perceived for polymer decomposition is the molecular weight. It has been observed that higher molecular weights result in lower catalytic reaction rates [22–24]. This could be due to higher viscosities associated with higher molecular weights and lower diffusion rates throughout the polymer melt. This work aims to understand what role the degrees of branching and unsaturation play on the reactivity of polyolefins over acid catalysts.

2. Materials and methods

2.1. Polymer samples

Additive-free HDPE (M_n ~20,000 Da) and LLDPE (M_n ~48,000 Da) samples were provided by Chevron Phillips Chemical in powder form. For the analysis of the effect of unsaturation, *hydrogenated HDPE* was prepared. The hydrogenation reactions were carried out in a Parr batch reactor equipped with a Teflon liner and a turbine-type impeller. Plastic, solvent and catalyst – 1.2 g HDPE, 40 g cyclohexane (suitable for HPLC, ≥99.9 %, acquired from Sigma Aldrich) and 600 mg Pd/Al_2O_3 (0.5 wt% Pd, 3.2 mm pellets, acquired from Sigma Aldrich) – were added to the reactor and the system was flushed with hydrogen. The reactor was pressurized to 300 psig H_2, stirring was set to 350 rpm, and the temperature was slowly ramped up to 150 °C. After the system reached the set temperature, the reaction was allowed to proceed for 1 h, under a total pressure of 380 psig. After quenching, the reactor was depressurized, and the catalyst pellets were separated out. Finally, the resulting hydrogenated HDPE was separated from the solvent, and dried overnight in a vacuum oven at 60 °C.

2.2. Polymer characterization

Molecular weights (MW) and molecular weight distributions (MWD) were obtained from high temperature gel permeation chromatography (GPC) using a PL 220 high temperature GPC/SEC unit (Agilent). Samples were dissolved in 1,2,4-tricholorobenzene (TCB) by heating at 150 °C for about 4 h with gentle, occasional stirring. BHT (2,6-di-tert-butyl-4-methylphenol) at a concentration of 0.5 g/L was used as a stabilizer in the TCB. An injection volume of 400 μL was used with a nominal polymer concentration of 0.5 mg/ml and a flow rate of 1.0 ml/min was maintained. Three Waters Styrogel HMW-6E columns were used and were calibrated with the integral method using a broad linear polyethylene standard (Chevron Phillips Chemical's Marlex® RTM BHB 5003 polyethylene resin) for which the molecular weight distribution had been determined. An IR4 detector (Polymer Char, Spain) was used for the concentration detection.

The concentration of various types of unsaturation in the polymer samples were quantified by a method based on proton nuclear magnetic resonance (NMR). [25–27] Polymer samples for NMR data collection were prepared by dissolving polymer powder samples in deuterated 1,1,2,2-Tetrachloroethane-d_2 (TCE-d_2, ≥ 99.5 atom %D). 0.035 g of powder of the polymer samples were added to 0.7 ml of TCE-d_2 solvent in a 5 mm NMR tube. The sample and solvent mixture was heated in a heating block at 130 °C for 4 – 5 h. The mixture was occasionally stirred with a stainless-steel stirrer to ensure homogeneous mixing. The resulting solution was then left overnight (for 15–16 h) in the heating block at 110 °C to ensure complete disentanglement of the polymer chains. The final concentration of the sample solutions was ~3.0 wt%. The NMR data were collected at 125 °C (398 K) in the Bruker 500 MHz NMR instrument fitted with a Bruker 5 mm BBI probe which was equipped with z-gradient. The sample was equilibrated inside the probe at 125 °C for 15 min before starting the data collection. Regular proton NMR data was collected with *zg* pulse sequence from Bruker's pulse program library using the following acquisition parameters: 5.0 s relaxation delay, 7.4 μs pulse width, 14 W pulse power, 4 dummy scans, 5.0 s acquisition time, 1024 scans and 9 ppm spectral window. The pre-saturation proton NMR data was collected with *zgpr* pulse sequence using the following acquisition parameters: 5.0 s relaxation delay, 7.4 μs pulse width, 14 W pulse power, 2.74×10^{-5} W pre-saturation pulse power, 4 dummy scans, 5.0 s acquisition time, 1024 scans and 20 ppm spectral window. The transmitter offset was placed at the center of the proton peak arising from the backbone proton atoms of polyethylene (PE) for efficient suppression of that peak. This PE backbone peak appears at ~1.35 ppm. All the data were processed with 0.3 Hz line broadening, zero filled with 4X of time domain data points and referenced to the residual proton peak of TCE-d_2 which was calibrated at 6.0 ppm. The data were collected and processed with Bruker's Topspin software (version 3.2 pl 6).

For ^{13}C NMR data collection, 0.55 g of polymer sample was dissolved in a mixture of 1,2,4-trichlorobenzene (TCB) and 1,4-dichlorobenzene-d_4 (DCB-d_4) solvents to achieve a concentration of ~10 wt%. The ^{13}C NMR spectra of the polyethylene samples were collected with standard pulse program using the standard parameter set including: a 13.0 μsec 90° pulse width, a 21.7 kHz spectral window, 7.0 s relaxation delay, 3.0 s acquisition time. 8k transients were collected in an overnight experiment and full NOE was exploited during data collection to improve the S:N ratio at a reasonable amount of time. The data was zero filled to 131k data points and exponentially weighted with a 1.0 Hz line-broadening before Fourier transformation. The spectrum was referenced to backbone -CH_2- peak which was calibrated at 30.0 ppm.

2.3. Catalyst samples

NH_4-ZSM-5 catalysts (framework type MFI), with Si/Al = 40 (CBV 8014) and Si/Al = 140 (CBV 28014), were obtained from Zeolyst International. To render them acidic, the zeolites were calcined under 40 ml/min of air (80 % N_2 / 20 % O_2) at 600 °C for 5 h, with a ramp rate of 2 °C/min. When used in flow reactors, the H-ZSM-5 was pelletized between 250 and 425 μm.

In order to assess diffusion properties, a core-shell zeolite (active ZSM-5 core, inert silicalite shell) was prepared based on the procedure described by Ghorbanpour et al. [28] In our work, however, we used Zeolyst MFI seeds to grow the silicalite layer, instead of synthesizing the zeolite entirely. Also, the annealing step was not performed, which considerably lowers the time necessary for this sample preparation. 750 mg of NH_4-ZSM-5 (Si/Al = 40) were added to a dilute growth solution – 1.3 ml tetraethyl orthosilicate (TEOS) 98 %, and 2.8 ml tetrapropylammonium hydroxide 40% in 65 ml of water, in which TEOS was added dropwise –, and left reacting at 100 °C for 24 h in a rotisserie oven. The mixture was then centrifuged, and the zeolite was washed with deionized water 5 times. The solids were dried in a vacuum oven overnight at 80 °C, and subsequently calcined under 40 ml/min air flow according to the following temperature program: 1 h isothermal at 350 °C (ramp rate = 1 °C/min) to clean the surface of any remaining water, followed by 5 h

Table 1
Polymer samples characterization. Short chain branching (SCB) and M_n were calculated from ^{13}C NMR data. M_n was determined via GPC, and unsaturation values were calculated from proton NMR data.

Sample	SCB /1000 C	M_n (Da)	M_w (Da)	Unsaturation /10^6 C				
				Vinylene *internal*	Trisub *internal*	Vinyl *terminal*	Vinylidene *terminal*	**Total**
LLDPE	16.6	48,190	112,150	108	87	40	15	250
HPDE	0.7	20,263	157,170	728	4	175	0	907

at 600 °C (ramp rate = 2 °C/min). The resulting catalyst is referred to as *ZSM-5 @Silicalite-1*.

Amorphous silica-alumina (ASA) catalyst support grade 135, Si/Al = 6, was obtained from Aldrich and used as received.

2.4. Catalyst characterization

The number of Brønsted acid sites (BAS) in the catalysts was determined by isopropylamine temperature-programmed reaction (IPA-TPRx) – the detailed procedure has been reported elsewhere [29]. Zeolites were imaged by a Zeiss Neon 40 EsB scanning electron microscope (SEM).

Nitrogen physisorption analysis was conducted using a TriStar II 3020. The samples were degassed under vacuum at 350 °C (ramp rate of 5 °C/min) for 10 h to remove moisture and volatile impurities. The catalyst weight was measured after degassing, and the samples were cooled down under liquid nitrogen for the adsorption-desorption analysis. Total surface areas and external surface areas were calculated using the Brunauer-Emmett-Teller (BET) method and the t-plot method, respectively.

To verify the formation of the silicalite shell on ZSM-5, two probe reactions were performed in a flow reactor: acetic acid ketonization at 320 °C, and triisopropylbenzene (TIPB) cracking at 400 °C. The reactor consisted of a 0.25-in. OD quartz tube in a furnace, and the products were analyzed in a Hewlett Packard 6890 gas chromatograph (GC) equipped with an INNOWax column (30 m × 0.25 mm × 0.25 μm) and a flame ionization detector (FID). Both inlet and outlet lines were heated to avoid condensation of reactants and products. Reactions were performed under a 62.5 ml/min flow of helium and using 35 mg of fresh catalyst. W/F was 0.2 h for TIPB cracking, and 0.3 h for acetic acid, where F is the reactant feed rate. The zeolites were pretreated under the same flow of helium at the reaction temperature for 1 h prior to the reaction start.

2.5. Polymer decomposition reactions

Reactions were carried out in a NETZSCH STA Jupiter 449 F1 thermogravimetric analysis (TGA) system, under 40 ml/min flow of argon. Catalyst powder, when used, was added to the bottom of the Al_2O_3 pan, and 20 mg of polymer sample were added on top of the catalyst.

For the product distribution analysis, 20 mg of polymer were mixed with the catalyst and packed in a quartz micropyrolysis tube. The micropyrolysis tube was then inserted into a 0.25 in. OD quartz tube, which was placed in a horizontal reactor furnace. This setup allows for the carrier gas to flow around the micropyrolysis tube, avoiding the polymer melt to plug the tube, which could cause overpressure. N_2 was used as the carrier gas, at a flow rate of 40 ml/min. The reactor temperature was increased from room temperature to 350 °C at a ramp rate of 2 °C/min, and the final temperature was held for 30 min. Gas bags were used to sample evolved products downstream of the reactor, and no condensation was observed in the bags after sampling. The gas samples were analyzed in a Shimadzu QP2010 GC-FID/MS system, equipped with a HP-PLOT/Al_2O_3/S column.

3. Results and discussion

The results of polymer samples characterization can be found in Table 1. HDPE and LLDPE were chosen to assess the importance of branching in the decomposition reaction due to their disparity in short chain branching (SCB): 0.7 vs. 16.6 per 1000 total carbon atoms. Hence, LLDPE has ~24 times more tertiary carbons per mole of carbon than HDPE does.

Fig. 1 shows the decomposition curves for HDPE and LLDPE at a temperature ramp rate of 5 °C/min up to 500 °C followed by holding the final temperature for one hour. It can be noticed that, when comparing thermal decomposition curves for both samples, LLDPE depolymerizes slightly faster than HDPE. This is likely because tertiary alkyl radicals are more stable than secondary alkyl radicals, and the rate limiting step for thermal pyrolysis is usually the initiation step [30] – hence, rates are slightly faster for the branched polymer.

The addition of 2 % catalyst reduces the temperature of maximum degradation by ~50 °C for both samples. However, the HDPE and LLDPE decomposition curves still overlap, indicating no significant difference in rates between these samples. Our group has discussed in a previous work [29] that performing polyethylene depolymerization at this ramp rate up to high temperatures (500 °C) did not allow for differences among catalysts to be noticed in the decomposition curve. Similarly, in this case, working at high temperature does not allow us to perceive differences in rate between these polyethylene samples.

The temperature ramp rate was then decreased to 2 °C/min, and the final (hold) temperature set to 350 °C. At this temperature, no significant decomposition occurs in the absence of catalyst, as can be seen in Fig. 2 (A and B). Three different acid catalyst samples – ZSM-5 (Si/Al = 40 and 140) and ASA – were used to decompose the two polyethylene samples. The catalyst loading was adjusted for each catalyst so that all the experiments were run with the same total number of Brønsted acid sites, as measured by IPA-TPRx (Fig. 2 C).

The results from Fig. 2 (A and B) display different behaviors of

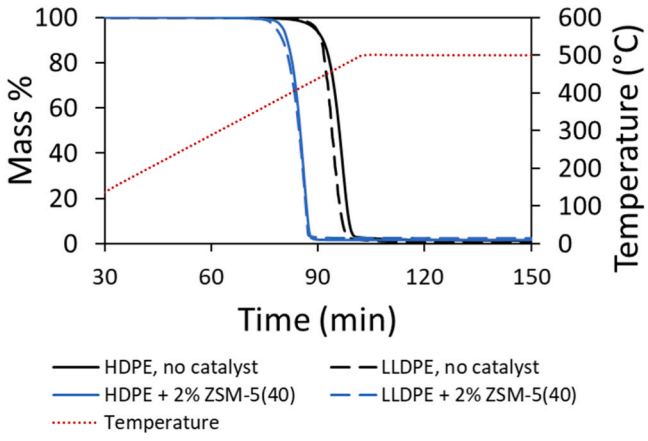

Fig. 1. TGA curves for HDPE (full lines) and LLDPE (dashed lines) decomposition under inert environment, thermally (black lines) and over 2 % ZSM-5 (Si/Al = 40, blue lines). Ramp rate = 5 °C/min up to 500 °C, followed by a 1-hour isothermal.

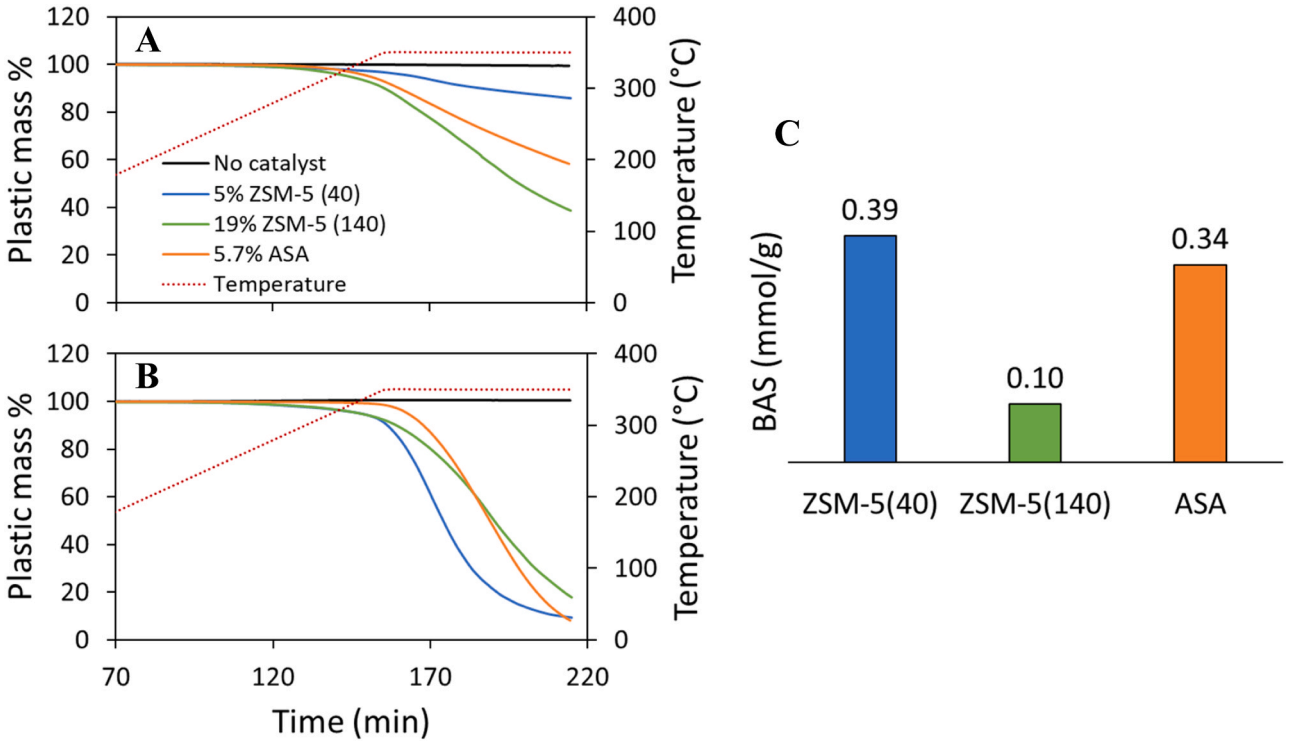

Fig. 2. TGA thermal and catalytic decomposition curves for (A) HDPE, and (B) LLDPE. Temperature ramp rate = 2 °C /min up to 350 °C, followed by a 1-hour isotherm. (C) Brønsted acid site density measured by IPA-TPRx.

catalytic degradation for both polymer samples. HDPE shows much lower conversion to gases than LLDPE after 1 h at 350 °C: HDPE reached 14 % conversion over ZSM-5 (40), 42 % over ASA, and 61 % over ZSM-5 (140); whereas LLDPE reached 91% conversion over ZSM-5 (40), 92 % over ASA, and 82 % over ZSM-5 (140). An interesting aspect of these experiments is that the activity of the catalysts followed different trends when using different reactants. For instance, ZSM-5 (140) was the most effective catalyst to convert HDPE; however, when used to decompose LLDPE, ZSM-5 (140) was the least effective catalyst. For easier comparison, curves for both polymer samples according to the type of catalyst are plotted in Fig. S1.

The HDPE curves suggest that cracking may be related to the total surface area available for the polymer to adsorb and react. Textural properties of the catalysts used can be found in Table 2. The effectiveness of the catalyst was correlated to the amount introduced to the system, and higher catalyst loadings (higher total surface areas) showed better performance. If we analyze the rates of weight loss (see Fig. S2) after the temperature reaches the set point and before the inflection point of the TG curve, we notice that the rates of reaction are about 4.1 times faster over MFI (140) vs. MFI (40) – this value roughly corresponds to the ratio of catalyst mass added to the system (0.19/0.05 = 3.8), since their specific surface areas are similar. Also, ZSM-5(140) contains fewer aluminum atoms on the external layer, decreasing the overall polarity of the external surface for this catalyst when compared to ZSM-5(40). Therefore, a strongly non-polar molecule such as polyethylene should have better interactions with a less polarized surface, where ensuing wettability and catalyst/polymer interaction is more favorable with Si/Al = 140 than with Si/Al = 40 which in turn will yield higher rates.

Amorphous silica alumina (ASA), added in a similar amount as ZSM-5(40), presents faster rates that are not simply proportional to the catalyst mass and consequent available surface area. This enhanced activity may be explained either by its mesoporous nature or surface polarity, or a combination of the two. The mesoporous structure of the ASA samples eases diffusion of the polymer into the catalyst particles and allows HDPE to access more acid sites per unit time. It is also important to note that zoning in MFI catalysts is common, often resulting in higher Al concentrations near the surface than in the bulk of the crystal [28,31]. This could imply that the exposed Al content on the MFI 40 catalyst near the surface could be a bit higher than the Si/Al ratio alone would suggest. Therefore, at a similar Si/Al ratio between MFI 40 and ASA, one might speculate that the surface Al content, and ensuing polarity on the surface may be higher for the former. This could result in decreased wettability with the hydrophobic HDPE polymer chains.

LLDPE decomposition curves, although consistently presenting conversions above 80%, seem to be related to the nature of the catalysts used. Faster rates (steeper inclinations) are achieved with higher acid densities (ZSM-5 40 and ASA). Although ASA possesses acid site densities comparable to those of ZSM-5 (40), its mesoporous nature and arguably weaker BAS (due to its amorphous nature and consequently larger Si-O-Al angles [32] when compared to zeolites) modify

Table 2
Textural properties of acid catalysts.

Sample	BET surface area (m^2/g)	External surface area* (m^2/g)	Total pore volume (cm^3/g)	Micropore volume* (cm^3/g)
ZSM-5(40)	398.6	113.8	0.231	0.128
ZSM-5(140)	372.7	111.2	0.224	0.114
ASA	509.4	556.9	0.666	0
ZSM-5(40)@Silicalite-1	384.1	106.8	0.205	0.119

*Obtained by t-plot method

polymer-catalyst interactions in such a way that the reaction onset takes longer to appear in the TG plot. It is possible, however, that cracking reactions are still happening at a similar rate but generating long-chain molecules that do not leave the polymer melt and thus cannot be detected by this technique, which would result in an apparent flat line in the TGA curve.

In order to assess the polymer's ability to diffuse into microporous catalysts, a core-shell ZSM-5 was prepared. The full procedure can be found in the Materials and Methods section, in which an inert, thin silicalite shell was grown on NH_4-ZSM-5 seeds. The purpose of these samples is to help reveal whether the polymer decomposition reactions happen preferentially on the external surface of the catalyst, or the polymer has the ability to diffuse into the microporous channels of the catalyst and access the majority of the acid sites.

IPA-TPRx reveals that the BAS density of the ZSM-5@Silicalite-1 sample is 0.39 mmol/g_{cat}, which is the same acidity as the parent zeolite (see Fig. 3). This, along with the practically unchanged BET surface area (see Table 2), suggests that there was no pore plugging due to deposition of silica. Also, the unchanged BAS density indicates that the silicalite layer is actually quite thin, as the formation of this layer did not add enough mass to decrease the BAS density of the sample. SEM images for ZSM-5 and ZSM-5 @Silicalite-1 also support this claim since the average particle size (~1 μm) is unchanged, as shown in Fig. S3.

Two probe reactions were used as proof of concept for the use of this ZSM-5@Silicalite-1: triisopropylbenzene (TIPB) cracking, which should occur only on the external sites of the catalyst due to shape selectivity constraints; and acetic acid ketonization, which should happen on any acid site of the zeolite since the reactants and products are significantly less bulky thus easily diffusing in and out of the catalyst particle. We note that these two probe reactions have been successfully employed previously to assess the content of internal vs. external acid sites in microporous materials.[28,33] The turnover frequencies (TOF) for each of these reactions can be found in Fig. 3. It is noticeable that the TOFs for TIPB cracking over ZSM-5 @Silicalite-1 are much lower than the ones over ZSM-5, corresponding to only ~5 % of the activity of the parent zeolite. This denotes that the external sites were successfully covered by the inert silicalite, and any activity on the external surface sites should be minimal. On the other hand, the TOFs for acetic acid ketonization are quite similar between the two catalysts: the activity over ZSM-5@Silicalite-1 was, on average, 90% of that over the parent zeolite. This small difference in activity may be due to mass-transfer limitations caused by pore narrowing due to silica deposition.

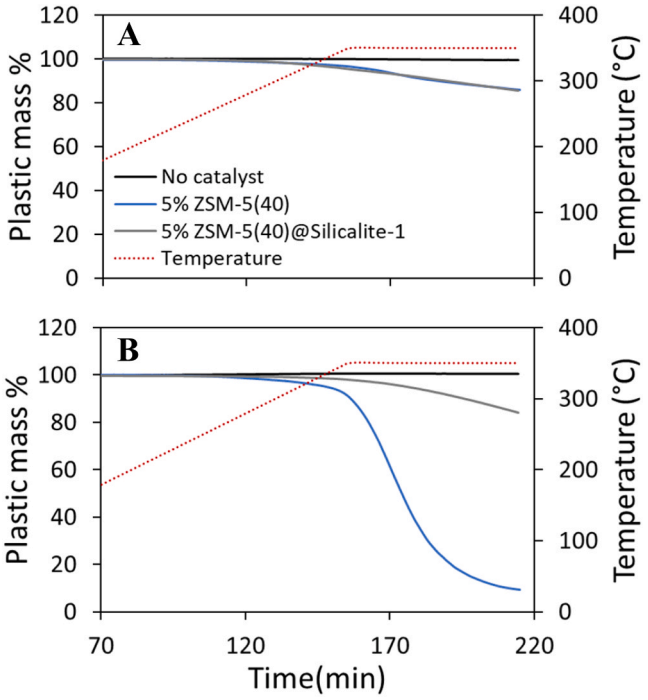

Fig. 4. TGA curves for polymer decomposition over 5% ZSM-5 (40) and ZSM-5 (40)@Silicalite-1 for (A) HDPE, and (B) LLDPE. Temperature ramp rate = 2 °C /min up to 350 °C, followed by a 1-hour isotherm.

When used to catalyze the polymer decomposition reaction, ZSM-5@Silicalite-1 shows two different behaviors for the different PE samples. As can be seen in Fig. 4, HDPE displays nearly identical decomposition curves over regular ZSM-5 and the core-shell catalyst. This

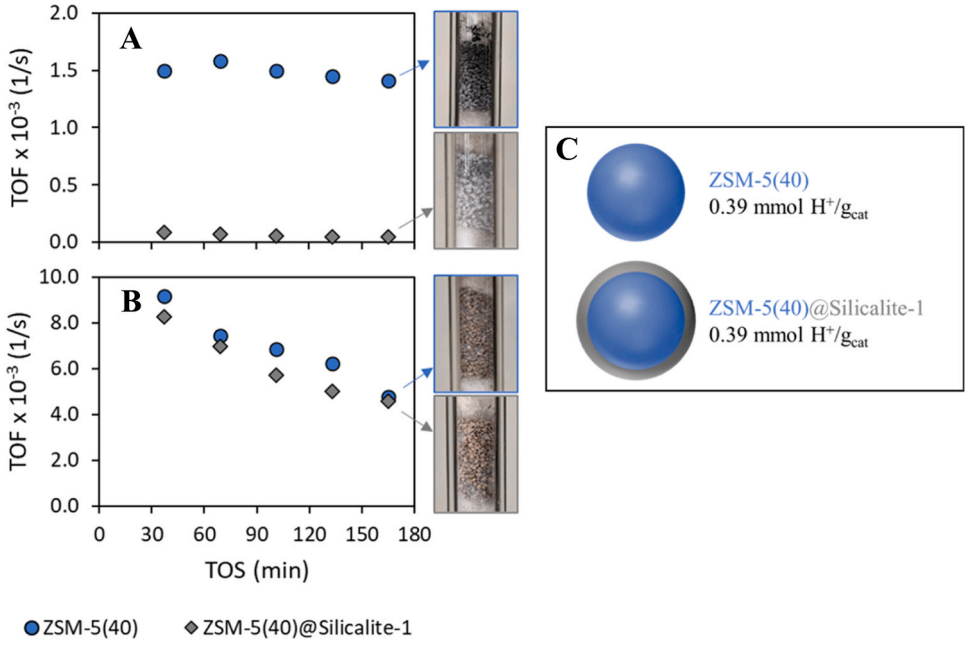

Fig. 3. Turnover frequencies (TOF, 1/s) vs. time on stream (TOS, min) in a flow reactor for (A) TIPB cracking at 400 °C, and (B) acetic acid ketonization at 320 °C. (C) Visual representation of ZSM-5 and ZSM-5 @Silicalite-1 (thickness of inert external shell is exaggerated for better visualization), and the BAS densities as measured by IPA-TPRx.

indicates that the external layer is not the only surface where the cracking reactions take place: if the polymer molecules can reach any acid site in the zeolite (internal or external), then the total rate should be dependent mostly on the internal sites, as they are more numerous than external ones. Hence, it can be concluded that this HDPE sample can successfully diffuse into the zeolite pores prior to cracking into smaller molecules.

The LLDPE sample, though, displays strikingly different rates over ZSM-5 @Silicalite-1 vs. ZSM-5. Whereas the parent zeolite is able to reach 91 % conversion to gases after 1 h of reaction, the silicalite shell catalyst is only able to reach 16% conversion by the end of the experiment. These curves denote that most of LLDPE decomposition reactions occur on the external sites of the zeolite, since the reaction is much suppressed when the external layer consists of inert silica.

One interesting finding that can be inferred from these experiments as well is the fact that the HDPE and LLDPE TGA profiles appear to be so similar over the silicalite-1 coated catalysts. Because we know that a) the intrinsic kinetic constant for LLDPE conversion over acid sites is significantly higher than HDPE conversion over acid sites, and b) the rate observed in these materials is proportional to both the rate constant and diffusivity of the polymer within the pores; one might infer that the rate of diffusion of HDPE through the hydrophobic silicalite shell, and possibly through the MFI framework, is faster than the LLDPE diffusion in hydrophobic MFI materials.

It is important to note that the diffusivity of polymer chains through the polymer melt itself may also play an important role in these experiments – the polymer molecules need to be able to reach the catalyst surface. The self-diffusion coefficient tends to be slightly lower for LLDPE when compared to HDPE; also, diffusivity decreases as molecular weight increases.[34] Both of these correlations lead to the conclusion that the self-diffusivity of LLDPE is lower than that for HDPE. Nonetheless, LLDPE displays much higher reactivity when the zeolite external layer is catalytically active – denoting the high importance of tertiary carbons for perceived rates.

The product distribution over ZSM-5 (140) at 350 °C can be found in Fig. 5. Products were comprised of olefins and paraffins in the range of C_2-C_7. No methane or aromatics were detected. Comparing the carbon number distributions, it is noticeable that the products from LLDPE are heavier than those coming from HDPE. This result is in agreement with the finding that HDPE is decomposed mostly in the internal BAS of MFI, whereas LLDPE decomposes primarily on the external surface. When bulky products are formed inside micropores, as is the case of the HDPE sample, there is a higher probability that they will further decompose into shorter chains during their diffusion out of the pores. [35] In contrast, when products are formed on external sites, they can easily diffuse out and move into the gas phase – this is likely the reason why the gas product formed from the decomposition of LLDPE is richer in the heavier fractions C_5, C_6 and C_7.

It can also be noticed that LLDPE produces more light alkanes (C_2-C_4) when compared to HDPE, which yields more light olefins. Total olefin-to-paraffin (O/P) ratio of the measured gas phase products was 2.1 for HDPE, and 1.5 for LLDPE. In these reactions, olefins are formed via beta-scission, as protolytic cracking typically requires higher temperatures to proceed. It might be expected that beta-scission would be faster for the branched LLDPE than for the linear HDPE, due to both the more facile initial protonation of tertiary carbons that are present in the former, as well as more stable carbenium ions formed as a result of beta-scission events due to the increased abundance of nearby branched hydrocarbons. Nevertheless, it is important to notice that given lower intrinsic barriers for isomerization when compared with beta-scission, isomerization reactions should readily occur for both samples, avoiding the production of unstable primary carbenium ion products in both reactions [35]. Because traditional beta-scission in the absence of sequential hydride transfer produces equimolar amounts of alkene and alkane products, the O/P ratio is therefore controlled not necessarily by initial reactivity, but by relative rates of beta-scission to other reactions such as hydride transfer. Further, multiple scission events can occur on the same polymer chain, resulting in O/P ratios of the light gas products greater than unity. Beta-scission produces a paraffin and a surface carbenium ion. Hydride transfer would lead to desorption of these surface species as paraffins as opposed to desorption as olefins. Hence, what controls the O/P ratio difference is not solely dictated by beta-scission rates, but by the ratio of beta-scission to other paraffin-producing reactions.

There are two main pathways in acid catalysis to generate paraffins: protolytic cracking and hydride transfer [36]. Nonetheless, protolytic cracking is only kinetically relevant at high temperatures and very low concentrations of alkene [37]. The reactions depicted in Fig. 5 were performed at considerably low temperature (350 °C), and the concentration of olefins is significant at 8 % conversion. Given that the formation of paraffins is then controlled by hydride transfer, one may conclude that hydride transfer occurs more significantly in LLDPE than in HPDE. This may be explained by the fact that branched hydrocarbons are better hydrogen donors than linear ones, since the resulting tertiary carbenium ion is more stable than a secondary one [38,39]; hence, activation energies are lower for hydride transfer to occur when branched paraffins are present, as is the case of the LLDPE chains.

To systematically study the role of the unsaturation inherently present in polyethylene samples, the HDPE sample was hydrogenated in order to generate a sample that had exactly the same properties as the original one (same molecular weight distribution and degree of branching) but contains a lower quantity of double bonds. MW

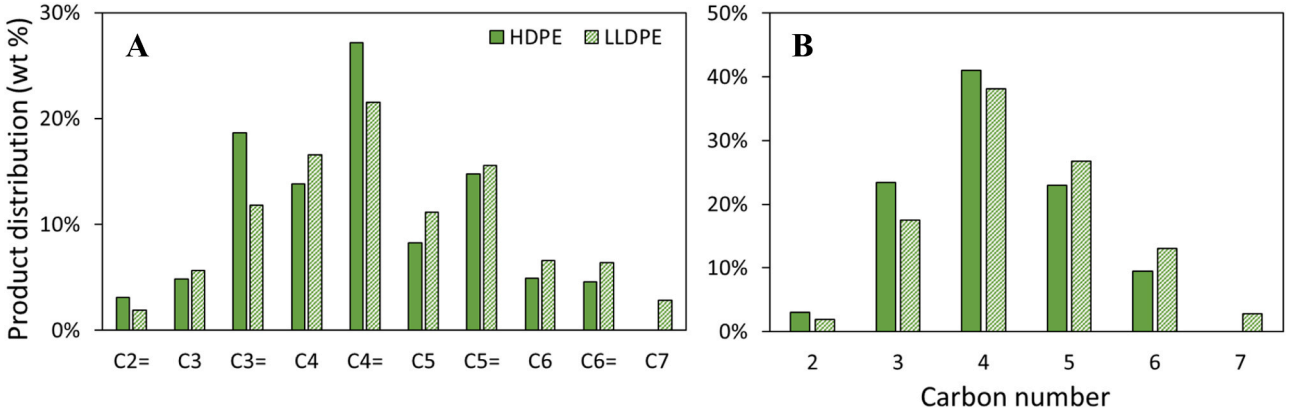

Fig. 5. (A) Product distribution for polyethylene samples over 19% ZSM-5 (140) at 350 °C. (B) Product distribution lumped by carbon number. Temperature ramp = 2 °C/min up to 350 °C, final temperature held for 30 min. Gas products were sampled at the moment when the temperature reached 350 °C. Conversion to gases = 8% at these conditions, according to TGA data.

Table 3
NMR unsaturation quantification comparing the original HDPE and hydrogenated HDPE samples.

Sample	Unsaturation /10^6 C				
	Vinylene *internal*	Trisub *internal*	Vinyl *terminal*	Vinylidene *terminal*	**Total**
HDPE	728	4	175	0	**907**
Hydrogenated HDPE (1 h)	102	0	98	0	**200**
Hydrogenated HDPE (5 h)	137	0	68	0	**205**
% reduction after 1-hour reaction	*86%*	*100%*	*44%*	-	***78%***
% reduction after 5-hour reaction	*81%*	*100%*	*61%*	-	***77%***

characterization comparing the original and hydrogenated sample can be found in Fig. S4, and Fig. S5 shows that there is no change in the melting point of the polymer after hydrogenation – both indicating that the nature of the polymer seems to be unchanged except for the degree of unsaturation. The HDPE sample was chosen for this study because it was the one that presented the highest degree of unsaturation (see Table 1).

Table 3 shows the NMR quantification of unsaturation in the original sample and the hydrogenated samples. Performing the hydrogenation reaction for 1 h reduced the total amount of unsaturation in the sample by 78 %. After 1 h, the hydrogenation reaction seems to have achieved equilibrium, since performing the reaction for 5 h yields the same total number of double bonds per 10^6 carbons. However, as the reaction is allowed to happen for a longer time, double bond isomerization decreases terminal vinyl groups and increases internal vinylene groups. This isomerization tendency has been previously reported in the literature when hydrogenating polyethylene samples via homogeneous catalysis [40].

Among the hydrogenated HDPEs, the 5-hour sample presented a vinyl/vinylene unsaturation ratio that was the closest to the original HDPE sample – this ratio was 0.24 for the original HDPE, 0.96 for the 1-hour hydrogenated HDPE, and 0.50 for the 5-hour hydrogenated HDPE. Therefore, TGA decomposition runs over 5 % ZSM-5 were performed for the hydrogenated HDPE (5 h), and the resulting curves can be seen in Fig. 6. The decomposition curves for the hydrogenated sample overlap with those of the original HDPE sample. This denotes that the presence of double bonds at the concentrations present in commercial polyethylene – about 1 double bond for every 1100 carbons in the chain – is not the controlling factor in the acid-catalyzed pyrolysis. If this cracking reaction were governed by the protonation of unsaturated carbons, then the perceived rates for the hydrogenated samples should be proportionally lower.

These results may suggest that the cracking of HDPE molecules is not limited by protonation of the polymer chain, or that the rates measured are in fact diffusion rates – hydrogenating double bonds should not detrimentally influence the overall diffusivity of these molecules. Comparing this data to the results from Fig. 3 (A), it is likely that the rates measured in Fig. 6 are in fact diffusion-controlled. Hence, removing double bonds does not affect the rate of weight loss.

4. Conclusions

We have compared HDPE and LLDPE samples for reactivity over ZSM-5 and amorphous silica alumina. LLDPE displayed much higher reactivity than HDPE, even though most cracking reactions for the linear low density sample occurred only on the external sites of the zeolite. HDPE decomposes mostly in the internal sites, but with much lower reactivity. The region where the cracking reactions take place (internal vs. external sites), in turn, is reflected in the product distribution arising from each of the polyethylene samples. LLDPE yields heavier and more paraffinic products, whereas HDPE generates lighter and more olefinic products. Further, comparison of rates over catalysts with varying surface properties suggests that the surface polarity influences polymer-catalyst interactions, with consequences on reaction rates, and that internal diffusion of HDPE is faster than LLDPE within the confined pores of MFI samples.

Hydrogenation experiments were carried out to determine whether the presence of double bonds governs the rate of catalytic cracking of HDPE. We found that lowering the unsaturation levels in the polyethylene sample had no discernible effect on the rate of decomposition.

These findings provide important insight into the factors that govern polyolefin reactivity over acid catalysts, which will support the development of more efficient and sustainable methods for chemically recycling or upcycling polymer waste.

Funding

This work was supported by Chevron Phillips Chemical.

CRediT authorship contribution statement

ACJ: Conceptualization, Methodology, Investigation, Validation, Resources, Visualization, Writing – Original Draft. **LT**: Methodology, Investigation, Writing – Review & Editing. **MM**: Investigation, Validation, Resources, Writing – Review & Editing. **MAGB**: Supervision, Project administration, Funding acquisition, Writing – Review & Editing. **RA**: Project administration, Funding acquisition, Writing – Review & Editing. **LL**: Conceptualization, Supervision, Project administration, Writing – Review & Editing. **SC**: Conceptualization, Supervision, Project

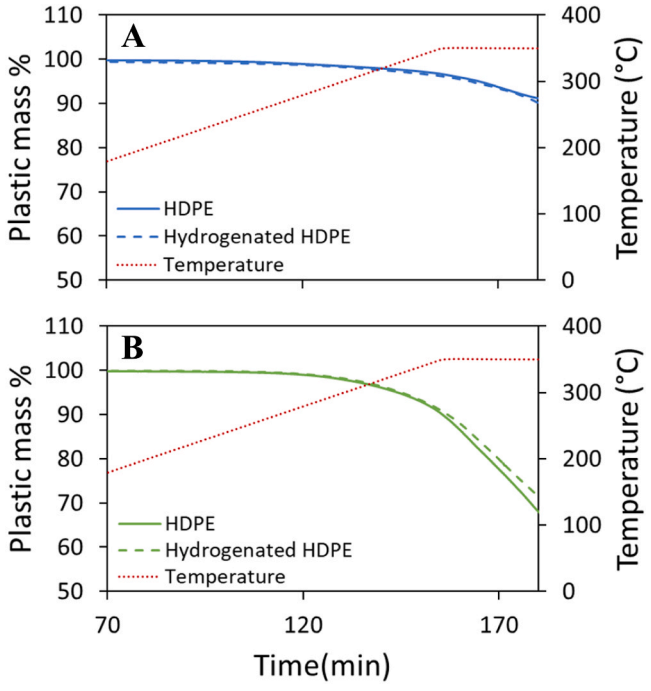

Fig. 6. TGA decomposition curves for HDPE and Hydrogenated HDPE (5 h) over (A) 5 % ZSM-5(40), and (B) 19 % ZSM-5(140). Temperature ramp rate = 2 °C /min up to 350 °C, followed by a 30-min. isotherm.

administration, Funding acquisition, Writing – Review & Editing.

Declaration of Competing Interest

The authors declare the following financial interests/personal relationships which may be considered as potential competing interests: Steven Crossley reports financial support was provided by Chevron Phillips Chemical Co LP. The work was sponsored by a research grant from CPChem, which resulted in this collaboration. The grant supports a GRA student stipend and reaction supplies. No other funds were provided as part of the grant/collaboration. SC.

Data availability

Data will be made available on request.

Acknowledgments

The authors would like to thank Steve Kelly for performing and discussing the BET experiments.

Appendix A. Supporting information

Supplementary data associated with this article can be found in the online version at doi:10.1016/j.apcatb.2023.122986.

References

[1] J.E. Rorrer, G.T. Beckham, Y. Román-Leshkov, Conversion of polyolefin waste to liquid alkanes with Ru-based catalysts under mild conditions, JACS Au 1 (2021) 8–12.
[2] S. Liu, P.A. Kots, B.C. Vance, A. Danielson, D.G. Vlachos, Plastic waste to fuels by hydrocracking at mild conditions, Sci. Adv. 7 (2021), eabf8283.
[3] I. Vollmer, M.J.F. Jenks, R. Mayorga González, F. Meirer, B.M. Weckhuysen, Plastic waste conversion over a refinery waste catalyst, Angew. Chem. Int. Ed. 60 (2021) 16101–16108.
[4] G. Celik, R.M. Kennedy, R.A. Hackler, M. Ferrandon, A. Tennakoon, S. Patnaik, A. M. LaPointe, S.C. Ammal, A. Heyden, F.A. Perras, M. Pruski, S.L. Scott, K. R. Poeppelmeier, A.D. Sadow, M. Delferro, Upcycling single-use polyethylene into high-quality liquid products, ACS Cent. Sci. 5 (2019) 1795–1803.
[5] G. Manos, A. Garforth, J. Dwyer, Catalytic degradation of high-density polyethylene over different zeolitic structures, Ind. Eng. Chem. Res. 39 (2000) 1198–1202.
[6] I. Vollmer, M.J.F. Jenks, M.C.P. Roelands, R.J. White, T. van Harmelen, P. de Wild, G.P. van der Laan, F. Meirer, J.T.F. Keurentjes, B.M. Weckhuysen, Beyond mechanical recycling: giving new life to plastic waste, Angew. Chem. Int. Ed. 59 (2020) 15402–15423.
[7] F. Zhang, M. Zeng, R.D. Yappert, J. Sun, Y.-H. Lee, A.M. LaPointe, B. Peters, M. M. Abu-Omar, S.L. Scott, Polyethylene upcycling to long-chain alkylaromatics by tandem hydrogenolysis/aromatization, Science 370 (2020) 437–441.
[8] A. Clark, J. Hogan, R. Banks, W. Lanning, Marlex catalyst systems, Ind. Eng. Chem. 48 (1956) 1152–1155.
[9] A.J. Martín, C. Mondelli, S.D. Jaydev, J. Pérez-Ramírez, Catalytic processing of plastic waste on the rise, Chem 7 (2021) 1487–1533.
[10] R.E. Harmon, G. SriBala, L.J. Broadbelt, A.K. Burnham, Insight into polyethylene and polypropylene pyrolysis: global and mechanistic models, Energy Fuels 35 (2021) 6765–6775.
[11] A. Marcilla, M.I. Beltrán, F. Hernández, R. Navarro, HZSM5 and HUSY deactivation during the catalytic pyrolysis of polyethylene, Appl. Catal. A: Gen. 278 (2004) 37–43.
[12] M.A. Uddin, K. Koizumi, K. Murata, Y. Sakata, Thermal and catalytic degradation of structurally different types of polyethylene into fuel oil, Polym. Degrad. Stab. 56 (1997) 37–44.
[13] D.W. Park, E.Y. Hwang, J.R. Kim, J.K. Choi, Y.A. Kim, H.C. Woo, Catalytic degradation of polyethylene over solid acid catalysts, Polym. Degrad. Stab. 65 (1999) 193–198.
[14] Y. Wang, Y. Zhang, H. Fan, P. Wu, M. Liu, X. Li, J. Yang, C. Liu, P. Bai, Z. Yan, Elucidating the structure-performance relationship of typical commercial zeolites in catalytic cracking of low-density polyethylene, Catal. Today 405-406 (2022) 135–143.
[15] G. Elordi, M. Olazar, G. Lopez, P. Castaño, J. Bilbao, Role of pore structure in the deactivation of zeolites (HZSM-5, Hβ and HY) by coke in the pyrolysis of polyethylene in a conical spouted bed reactor, Appl. Catal. B: Environ. 102 (2011) 224–231.
[16] D.P. Serrano, J. Aguado, J.M. Escola, Catalytic cracking of a polyolefin mixture over different acid solid catalysts, Ind. Eng. Chem. Res. 39 (2000) 1177–1184.
[17] D.P. Serrano, J. Aguado, J.M. Escola, J.M. Rodriguez, A. Peral, Catalytic properties in polyolefin cracking of hierarchical nanocrystalline HZSM-5 samples prepared according to different strategies, J. Catal. 276 (2010) 152–160.
[18] J. Aguado, D.P. Serrano, G.S. Miguel, J.M. Escola, J.M. Rodríguez, Catalytic activity of zeolitic and mesostructured catalysts in the cracking of pure and waste polyolefins, J. Anal. Appl. Pyrolysis 78 (2007) 153–161.
[19] F.C. Jentoft, B.C. Gates, Solid-acid-catalyzed alkane cracking mechanisms: evidence from reactions of small probe molecules, Top. Catal. 4 (1997) 1–13.
[20] V.B. Kazansky, Adsorbed carbocations as transition states in heterogeneous acid catalyzed transformations of hydrocarbons, Catal. Today 51 (1999) 419–434.
[21] R.J. Conk, S. Hanna, J.X. Shi, J. Yang, N.R. Ciccia, L. Qi, B.J. Bloomer, S. Heuvel, T. Wills, J. Su, A.T. Bell, J.F. Hartwig, Catalytic deconstruction of waste polyethylene with ethylene to form propylene, Science 377 (2022) 1561–1566.
[22] J.E. Rorrer, C. Troyano-Valls, G.T. Beckham, Y. Román-Leshkov, Hydrogenolysis of polypropylene and mixed polyolefin plastic waste over Ru/C to produce liquid alkanes, ACS Sustain. Chem. Eng. 9 (2021) 11661–11666.
[23] A. Thevenon, I. Vollmer, Towards a cradle-to-cradle polyolefin lifecycle, Angew. Chem. Int. Ed. 62 (2023), e202216163.
[24] B.C. Vance, P.A. Kots, C. Wang, J.E. Granite, D.G. Vlachos, Ni/SiO2 catalysts for polyolefin deconstruction via the divergent hydrogenolysis mechanism, Appl. Catal. B: Environ. 322 (2023), 122138.
[25] V. Busico, R. Cipullo, N. Friederichs, H. Linssen, A. Segre, V. Van Axel Castelli, G. van der Velden, H. NMR, analysis of chain unsaturations in ethene/1-octene copolymers prepared with metallocene catalysts at high temperature, Macromolecules 38 (2005) 6988–6996.
[26] Y. He, X. Qiu, J. Klosin, R. Cong, G.R. Roof, D. Redwine, Terminal and internal unsaturations in poly (ethylene-co-1-octene), Macromolecules 47 (2014) 3782–3790.
[27] T.J. Hermel-Davidock, M. Demirors, S.M. Hayne, R. Cong, Ethylene-based polymer compositions, Google Patents, 2013.
[28] A. Ghorbanpour, A. Gumidyala, L.C. Grabow, S.P. Crossley, J.D. Rimer, Epitaxial growth of ZSM-5@silicalite-1: a core–shell zeolite designed with passivated surface acidity, ACS Nano 9 (2015) 4006–4016.
[29] A.C. Jerdy, T. Pham, M.Á. González-Borja, P. Atallah, D. Soules, R. Abbott, L. Lobban, S. Crossley, Impact of the presence of common polymer additives in thermal and catalytic polyethylene decomposition, Appl. Catal. B: Environ. 325 (2023), 122348.
[30] X. Zhou, L.J. Broadbelt, R. Vinu, Chapter Two - Mechanistic understanding of thermochemical conversion of polymers and lignocellulosic biomass, in: K.M. Van Geem (Ed.), Advances in Chemical Engineering, Academic Press, 2016, pp. 95–198.
[31] R. Althoff, B. Schulz-Dobrick, F. Schüth, K. Unger, Controlling the spatial distribution of aluminum in ZSM-5 crystals, Microporous Mater. 1 (1993) 207–218.
[32] J.A. van Bokhoven, B.A. Williams, W. Ji, D.C. Koningsberger, H.H. Kung, J. T. Miller, Observation of a compensation relation for monomolecular alkane cracking by zeolites: the dominant role of reactant sorption, J. Catal. 224 (2004) 50–59.
[33] A. Corma, U. Diaz, V. Fornés, J.M. Guil, J. Martínez-Triguero, E.J. Creyghton, Characterization and catalytic activity of MCM-22 and MCM-56 compared with ITQ-2, J. Catal. 191 (2000) 218–224.
[34] G. Fleischer, The chain length dependence of self-diffusion in melts of polyethylene and polystyrene, Colloid Polym. Sci. 265 (1987) 89–95.
[35] S.P. Crossley, D.E. Resasco, G.L. Haller, Clarifying the multiple roles of confinement in zeolites: from stabilization of transition states to modification of internal diffusion rates, J. Catal. 372 (2019) 382–387.
[36] A. Corma, P.J. Miguel, A.V. Orchillés, Can macroscopic parameters, such as conversion and selectivity, distinguish between different cracking mechanisms on acid catalysts? J. Catal. 172 (1997) 355–369.
[37] S. Kotrel, H. Knözinger, B.C. Gates, The Haag–Dessau mechanism of protolytic cracking of alkanes, Microporous Mesoporous Mater. 35–36 (2000) 11–20.
[38] A.T. To, D.E. Resasco, Hydride transfer between a phenolic surface pool and reactant paraffins in the catalytic cracking of m-cresol/hexanes mixtures over an HY zeolite, J. Catal. 329 (2015) 57–68.
[39] P.V. Shertukde, G. Marcelin, G.A. Sill, W. Keith Hall, Study of the mechanism of the cracking of small alkane molecules on HY Zeolites, J. Catal. 136 (1992) 446–462.
[40] D. Witt, J. Hogan, Double-bond isomerization and hydrogenation in polyethylene with soluble nickel catalysts, J. Polym. Sci. Part A-1: Polym. Chem. 8 (1970) 2689–2701.